Pressure-volume-temperature dependence of poly-ε-caprolactam/clay nanocomposites

Utracki, L. A.; Simha, R.; Garcia-Rejon, A.

National Research Council Canada   Conseil national de recherches Canada

Canada

Pressure−Volume−Temperature Dependence of Poly-ε-caprolactam/Clay Nanocomposites

L. A. Utracki,*,† R. Simha,‡ and A. Garcia-Rejon†,§

National Research Council Canada, Industrial Materials Institute, 75 de Mortagne, Boucherville, QC, Canada, J4B 6Y4, and Department of Macromolecular Science and Engineering, Case Western Reserve University, Cleveland, Ohio 44106-7202

ABSTRACT: The pressure−volume−temperature (*PVT*) dependence of commercial poly-ε-caprolactam melt (PA-6) and based on it a nanocomposite containing 1.6 wt % of exfoliated montmorillonite (PNC) as well as their 1:1 mixture was determined at $T = 300-560$ K and $P = 0-150$ MPa. Incorporation of clay into PA-6 resulted in lowering the specific volume of PNC by about 1.0%. For all three molten resins excellent agreement between experiment and the results from Simha−Somcynsky lattice−hole theory was found. The hole (free volume) fraction, a sensitive indicator of structural changes, shows a pressure-dependent reduction of ca. 14−15% in PNC as compared with the neat PA-6. An evaluation of the binary interactions from the computed mean scaling parameters of the theory requires definition of the constituents. On the basis of experimental and computer simulation results in the literature, the following model was adopted: Flat disk particles of specified diameter are covered with a uniform layer of solidified PA-6 of specified thickness, thus forming "hairy" clay platelets (HCP). The remainder of PA-6 constitutes the matrix. Its mobility and other properties vary with the distance from the clay surface in the normal direction and reach as an asymptotic limit bulk values. Thus, the characteristic interaction parameters of the matrix vary with the interparticle distance and hence with clay content. The estimated cross-interaction parameters are appropriate averages of the two self-interaction quantities.

I. Introduction

The pressure−volume−temperature (*PVT*) equation-of-state (eos) properties of polymeric systems have been measured to predict their behavior when subjected to pressure and temperature variation during processing of such materials and thus to determine compressibility and the thermal expansion coefficient. However, by means of an adequate theory, the *PVT* relation may provide an insight into intermolecular attractions and repulsions in single-component as well as in multicomponent systems, such as solutions, blends, or composites. Furthermore, these properties are related to the free volume content, thus providing information on a wide range of properties related to it, viz. flow behavior, physical aging, elastic moduli, etc. Several comprehensive reviews of the eos's used for polymeric liquids have been published. For example, Rodgers collected *PVT* data for 56 polymers at $P \leq 200$ MPa and T ranging from 50 to 150 °C.[1] The review presents fundamentals of the theories, and it evaluates the fit to experimental data.

Recently, Simha et al. reported preliminary results of the *PVT* studies for poly-ε-caprolactam (PA-6) and the corresponding nanocomposite, containing 1.6 wt % of exfoliated montmorillonite (MMT).[2] These first published studies on the *PVT* behavior of the polymeric nanocomposites (PNC) showed that incorporation of exfoliated MMT does not significantly modify the general *PVT* behavior of the matrix polymer. Thus, the experimental data for polymer and PNC were fitted to Simha−Somcynsky (S−S)[3] eos with similar accuracy.[2]

† National Research Council Canada, Industrial Materials Institute.
‡ Case Western Reserve University.
§ Deceased March 2002.
* Corresponding author: E-mail leszek.utracki@cnrc-nrc.gc.ca.

The S−S theory is unique as it explicitly includes a free volume function, h. The preliminary data showed that, by comparison to the matrix, incorporation of MMT reduced h by about 14%. The theory describes the interactions within the system in terms of the two Lennard-Jones potential related parameters, i.e., the maximum attractive energy between a pair of chain segments, ϵ^*, and the corresponding segmental repulsion volume, v^*. For binary systems six parameters need to be determined (11, 12, and 22 for ϵ^* and v^*). To compute these parameters from the *PVT* data, the PNC was assumed to be composed of neat PA-6 matrix (with properties identical to the independently measured resin) and bare, randomly dispersed clay platelets.

The present publication summarizes extensive test results on three systems: the same PA-6 and PNC as described in the preliminary report[1] as well as their 1:1 mixture. The new set of data showed an inadequacy of the previous treatment. A new model is being proposed.

II. Experimental Section

Two commercial resins from Ube Industries Ltd., PA-1015B and PA-1015C2, were used. According to received information, the former was neat PA-6 and the latter based on it a nanocomposite containing 2 wt % organoclay (i.e., 1.6 wt % clay or 0.64 vol % clay). The molar mass of PA-6 in both systems was $M_n = 22$ kg/mol. In the following text these resins will be labeled as PA and PNC, respectively. The exfoliation in PNC concluded from the X-ray diffraction (XRD) and transmission electron microscopy (TEM)[4] studies were confirmed by TEM on the "as-received" and extruded specimens.

The two resins, PA and PNC, were melt-blended at a weight ratio 1:1 using a Leistritz twin-screw extruder (TSE), $D = 34$ mm, $L/D = 40$, in corotating mode, with the high-shear screw configuration at $T = 240$ °C. For this reason, PA and PNC were also reextruded. Thus, the *PVT* measurements were carried out on five samples: PA and PNC, virgin and reextruded, as well as on their 1:1 blend. Thus, the 1:1 mixture contains 0.8 wt % or 0.32 vol % of MMT.
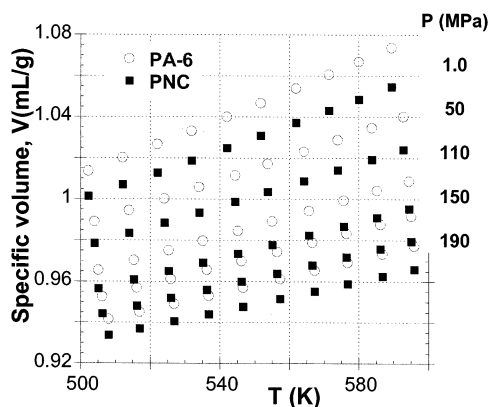
Figure 1. Specific volume for PA-6 and PNC vs temperature at indicated five pressures: ambient, then 50, 110, 150, and 190 MPa.

The *PVT* behavior was measured in a Gnomix apparatus (Gnomix Inc., Boulder, CO) within a range of temperatures ($T = 300-590$ K) and pressures ($P = 0.1-200$ MPa). The molten state was observed within the temperature range from about 500 to 590 K. Prior to testing, the material was dried for 48 h at 80 °C. Since the instrument measures only the incremental changes of the specific volume as a function of P and T, first an absolute value of the specific volume at ambient condition was measured with accuracy of $\Delta V \leq \pm 0.001$ mL/g. Considering the high hygroscopicity of PA, all manipulations with the resin were performed in a glove compartment under positive pressure of dry N_2.

For each resin at least six runs were carried out, two isobaric and the others isothermal. Furthermore, some of these runs were repeated up to three times. "Isobaric" means that at each level of pressure the volume changes in full range of T were carried out; then the next level of P was set and the process repeated. Similarly, during the "isothermal" runs the temperature was set and $V = V(P)$ was determined; then T was changed and the process repeated. Thus, in "isobaric" mode the specimen was exposed to the highest temperature as many times as the number of selected P levels (e.g., 10), whereas in "isothermal" runs the specimen was exposed to it only once, but for a longer period (required for measuring the volume changes at all P levels). Owing to the thermal decomposition at higher temperatures, the reproducibility between these two types of measurements was poor—worse for PNC than for PA. For this reason only single sweep, isothermal data were considered reliable.

To illustrate the effect of clay on specific volume, Figure 1 shows the $V = V(P,T)$ dependence for PA and PNC. To avoid crowding the figure, only five pressures are exhibited. In the full range of independent variables the ratio $V(PA)/V(PNC) = 1.013 \pm 0.004$. This compares well with the value 1.016 calculated from the known density of components, assuming volume additivity.

III. Theory: Single Constituent

The Simha–Somcynsky lattice–hole theory describes an amorphous assembly of chain molecules on a lattice with sites occupied by chain segments. In addition, to simulate molecular disorder, there is a fraction h of vacancies, which is a type of free volume quantity. The configurational thermodynamic properties, such as the *PVT* (eos) relations or the cohesive energy density, are then characterized by three quantities, i.e., the maximum attraction, ϵ^*, between a pair of chain segments, the corresponding segmental repulsion volume, v^*, and the number $3c$ of volume-dependent, external degrees of freedom. In terms of these quantities and the number s of segments per chain, the three characteristic pres-

sure, temperature, and volume parameters can be defined, viz.

$$P^* = zq\epsilon^*/(sv^*); \quad T^* = zq\epsilon^*/Rc; \quad V^* = v^*/M_s \quad (1)$$

with M_s the molar segmental mass, $zq = s(z - 2) + 2$, the number of interchain contacts in a lattice of coordination number $z = 12$, and R the gas constant. The variables of state, P, T, V, are then scaled by P^*, T^*, V^*, to define a universal, reduced $\tilde{P}-\tilde{T}-\tilde{V}$ surface, common to all liquids. Provided the theory is quantitatively successful, a superposition of experimental and theoretical lines yields the scaling parameters and thus the characteristic quantities defined in eq 1.

The S–S theory yields a reduced free energy function, $\tilde{F}$, as

$$\tilde{F} = \tilde{F}[\tilde{V},\tilde{T},h(\tilde{V},\tilde{T})] \quad (2)$$

According to eq 2, $\tilde{F}$ depends on reduced volume, $\tilde{V}$, reduced temperature, $\tilde{T}$, and the hole fraction h, which in turn varies with $\tilde{V}$ and $\tilde{T}$. The latter dependence is obtained by minimizing the free energy at a specified volume and temperature, i.e.

$$(\partial\tilde{F}/\partial h)_{\tilde{V},\tilde{T}} = 0 \quad (3)$$

Finally the reduced pressure is obtained as

$$\tilde{P} = -(\partial\tilde{F}/\partial\tilde{V})_{\tilde{T}} \quad (4)$$

The solution of eq 4 yields the eos:

$$\tilde{P}\tilde{V}/\tilde{T} = (1 - \eta)^{-1} + 2yQ^2(1.011Q^2 - 1.2045)/\tilde{T} \quad (5)$$

with $y = 1 - h$, $Q = 1/(y\tilde{V})$, and $\eta = 2^{-1/6}yQ^{1/3}$. The minimization condition, eq 3, yields the second relation:

$$3c[(\eta - {}^1/_3)/(1 - \eta) - yQ^2(3.033Q^2 - 2.409)/6\tilde{T}] + (1 - s) - sln[(1 - y)/y] = 0 \quad (6)$$

A further assumption for macromolecules ($s \gg 1$) has been usually employed, i.e., $3c/s \rightarrow 1$. Equations 5 and 6 have been applied to over 50 polymer and copolymer melts, and the scaling parameters, eq 1, have been tabulated.[1]

A simplification of the general relations 5 and 6 has been recently published.[5] Explicit polynomial interpolation expressions for $\tilde{V}$, the h-function and the cohesive energy density, CED, have been formulated in the full range of the reduced independent variables:

$$1.6 < 100\tilde{T} < 7.1 \quad \text{and} \quad 0 < 100\tilde{P} < 35$$

For example, the reduced volume can be written as

$$\ln \tilde{V} = a_0 + a_1\tilde{T}^{3/2} + \tilde{P}[a_2 + (a_3 + a_4\tilde{P} + a_5\tilde{P}^2)\tilde{T}^2] \quad (7)$$

The goodness of fit may be judged by the values of the standard deviation ($\sigma \leq 0.0018$) and the correlation coefficient squared ($r^2 \geq 0.9997$). Taking appropriate derivatives leads to the compressibility and the thermal expansion coefficients.

The determination of the reducing parameters from experimental data proceeds by simultaneous fit of eqs 5 and 6. The computations have been performed using MicroMath Scientist commercial software, which mini-

mizes the differences between the experimental data and the theory by the nonlinear least-squares algorithm.

IV. Theory: Two-Component System

Jain and Simha[6] extended the single-component theory to two component mixtures. Under random mixing assumptions, the scaled eqs 5 and 6 retain their formal validity, but the interaction parameters ϵ^* and v^* are replaced by compositional averages over "11", "22", and "12" interactions, $\langle \epsilon^* \rangle$ and $\langle v^* \rangle$. These averages $\langle \epsilon^* \rangle$ and $\langle v^* \rangle$ are related to the individual interactions as follows:

$$\langle \epsilon^* \rangle \langle v^* \rangle^p = X_1^2 \epsilon_{11}^* v_{11}^{*\,p} + 2 X_1 X_2 \epsilon_{12}^* v_{12}^{*\,p} + X_2^2 \epsilon_{22}^* v_{22}^{*\,p};$$
$$p = 2,4 \quad (8)$$

In eq 8 the site fractions X_1 and $X_2 = 1 - X_1$ are defined in terms of the mole fractions x_i as

$$X_1 = zq_1 x_1/(zq_1 x_1 + zq_2 x_2) \quad (9)$$

The two powers of p in eq 8 reflect the assumed $6-12$ pair potential. Thus, six interaction parameters of the theory are interrelated by the two relations in eq 8. In essence, to fully describe the *PVT* dependence of two-component systems, four sets of information are needed; these are either separate experiments at different concentrations or assumptions consistent with the lattice-hole model.

V. Model of Molten PNC

The model proposed in this paper is based on three sets of information: (1) The reduction of molecular mobility near a crystalline surface, as computed from molecular dynamics and experimentally measured. (2) The molecular structure of Ube PNC. (3) The *PVT* behavior of PA, PNC, and their mixture: PA:PNC = 1:1.

(1) Fleer et al. pointed out that any interface between phases induces changes in properties.[7] Thus, polymer adsorbed from a solution on a crystalline solid forms a layer whose thickness is comparable to the radius of gyration, $\langle s_\theta^2 \rangle^{1/2} = 5-35$ nm. The model computations indicate that, in the absence of direct chemical bonding, macromolecules physically adsorb on a solid surface by direct contact of several statistical segments labeled "trains", with loops and tails whose size depends on molecular weight, solvent, temperature, etc. Earlier studies by Cosgrove et al. of polymer adsorption on solids from dilute solutions indicated that homopolymer concentration exponentially decreases in the direction normal to the surface, z.[8,9] The root-mean-square (rms) thickness was slightly larger than the unperturbed radius of gyration, viz. 9.0 vs 6.8 nm for PS. Furthermore, the measurably higher than bulk concentration extended for at least 24 nm.

Israelachvili et al.[10] and Horn and Israelachvili[11] used the surface force balance instrument to measure the viscosity of PS solutions in cyclohexane near the Θ-condition. A solidlike behavior was reported for the first $2-9$ nm thick surface layer and progressive reduction of viscosity in the z-direction to the bulk solution viscosity for a distance $z_c = 60-120$ nm. The force measurements for PDMS squeezed between two mica plates showed a solidlike behavior for $z \leq 4$ nm and exponentially decreasing viscosity toward the bulk value at a distance of about 17 nm. Luengo et al.[12] studied the rheology of undiluted polybutadiene (PBD, M_w = 6.95 kg/mol) in a redesigned surface force balance. Two regions in steady-state flow were observed: (a) an incompressible "hard wall" at $z_{hw} \cong 5$ nm of solidlike PBD adsorbed on the mica surface and (b) a roughly exponential decay at larger distances. The dynamic oscillatory measurements identified three regions: bulk behavior for $z > 100$ nm, intermediate, and solidlike for $z \leq 6$ nm, where Hookean-type response of an elastic body was obtained.

Strong adsorption by a crystalline surface is not limited to macromolecules. Low molecular weight organic compounds having either spherical or short-chain molecules show a similar behavior.[13] For example, when dodecane is confined to a diminishing gap from ca. 5 to 2.8 nm, it undergoes an abrupt solidification. The process is rate-dependent; thus, the measured thickness of solidified layers varied from two molecular layers up. The adsorption caused the shear viscosity to increase by up to 7 orders of magnitude. Similar behavior has been computed using molecular modeling.[14] The author reviewed adsorption induced by chemical or physical interactions.

(2) According to an early patent, preparation of PNC involved three steps:[15] (a) intercalation of MMT with ω-dodecanoic acid ammonium chloride, (b) mixing the intercalated clay with ϵ-caprolactam and water, and (c) polymerization followed by pelletization. Excellent clay exfoliation was obtained. Later it was discovered that intercalated clay might be directly swollen by molten ϵ-caprolactam. Polymerization resulted in well-dispersed clay platelets in PA-6 matrix. At 2 wt % of organoclay loading, the matrix modulus increased by a factor of 1.5, the HDT increased from 75 to 140 °C, and the moisture permeability was reduced by half.[16,17] However, as a result of this procedure, all macromolecules were end-tethered to clay platelets through the amine end group; thus, the resulting PNC could not be colored by the traditional method. The following patent modified the process.[18] Thus, PNC is prepared by intercalation of MMT with 12-aminododecanoic acid and ϵ-caprolactam and then compounding the adduct in a twin-screw extruder with ca. 70% of PA-6. Chain-end titrations indicate that about $1/3$ of macromolecules are end-tethered, what eliminates the dyeability problem.

(3) The data reported in this articles have been collected with painstaking care over 15 months, investigating all possible influences, sources of error, and ad nauseam verifying the reproducibility. The new sets of data for PA and PNC virtually confirmed the accuracy of the preliminary findings[2] and lead to similar values of the interaction parameters. However, calculation of the binary interaction parameters using all three compositions (PA, PNC, and their 1:1 mixture) did not offer consistent solutions. For example, using the previous method of data treatment, different pairs of samples (e.g., PA with PNC, PA:PNC = 1:1 mixture with PA or PNC) produced different values of the binary interaction parameters. Evidently, the assumption of random mixing of "dry" platelets and neat bulk polymer is not valid for PNC, and a different model of molecular structure must be proposed.

The new model considers that in PNC: (1) One-third of clay cations are used for end-tethering the PA-6 macromolecules. (2) As shown in Figure 2, on all clay platelet surfaces there is an *inner* layer of solidified PA-6, $z_{sw} = 6$ nm, followed by an *intermediate* layer, $6 \leq z_{in}$ (nm) ≤ 100, where the segmental mobility of PA-6 chain
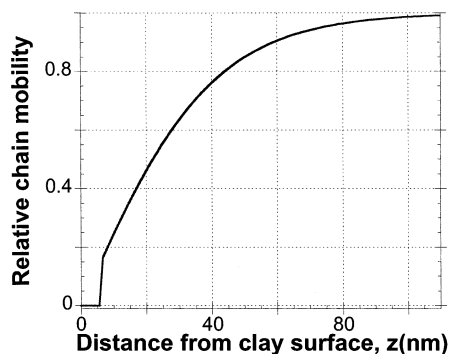
Figure 2. Relative segmental mobility of macromolecules as a function of the normal distance from the clay surface. The solidified macromolecules occupy the first 6 nm. The intermediate layer: $6 \leq z_{in}$ (nm) ≤ 100; while the exterior: $z > 100$ nm.

progressively increases to that in the *exterior* layer at $z > 100$ nm.

While the qualitative HCP image of PNC follows the results from the surface balance experiments and the computer simulation, someone may take issue with the adopted numerical values for z_{sw} and z_{in}. Considering the fact that the data were reported for solutions and for melts, the reported values for these quantities have been remarkably similar. In the absence of directly measured ones for the MMT/PA-6 pair the adopted values are reasonable. However, these parameters are used to calculate the PNC composition and the limits above which the "hairy" clay platelets (HCP) domains start to overlap. As will be evident from the numerical analysis of data, the calculated compositions are consistent with the experimental observations. While selection of other values for z_{sw} and z_{in} would lead to somewhat different compositions, nevertheless the physics would be the same.

The HCP model[19] implies that in the diluted system with the volume fraction $\phi < 0.005$, where the clay platelets are more than 200 nm apart, individual HCP's are dispersed in a matrix composed of PA-6 macromolecules that belong to intermediate and exterior layers. Thus, the values of the interaction parameters are expected to be constant. On the other hand, at higher concentrations, $\phi > 0.005$ (or $w > 1.2$ wt %), the domains of reduced mobility around HCP overlap, PA-6 macromolecules with "normal" bulk properties are absent, and the interactions depend on composition.
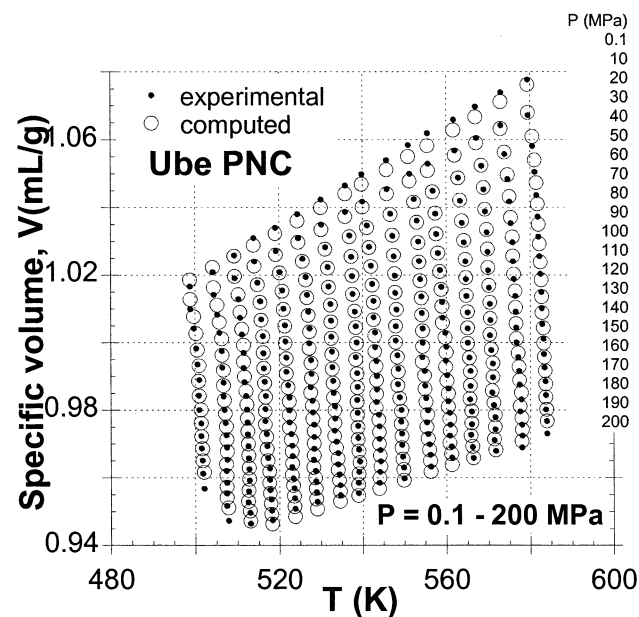
VI. Calculations

Figures 3 and 4 illustrate the ability of eqs 5 and 6 to describe the *PVT* behavior for PA-6 and PNC, respectively. It is understood that in the latter these equations may be formally applied, but the interpretation of the average scaling parameters is left open. Similarly good agreement of theory with experiment was observed for the PA/PNC = 1:1 mixture. The statistics of the analysis yields the results shown in Table 1.

Out of five measured polymeric species only three are presented in Table 1—it was found that within limit of experimental error the data for extruded and virgin PA or PNC resins show the same behavior. The first three rows in Table 1 provide the error statistics for the least-squares fitting of eqs 5 and 6 to the experimental data. Very few *PVT* tests gave larger standard deviation $\sigma > 0.0014$ or the correlation coefficient squared $r^2 < 0.999\ 996$. The middle four rows of Table 1 list the
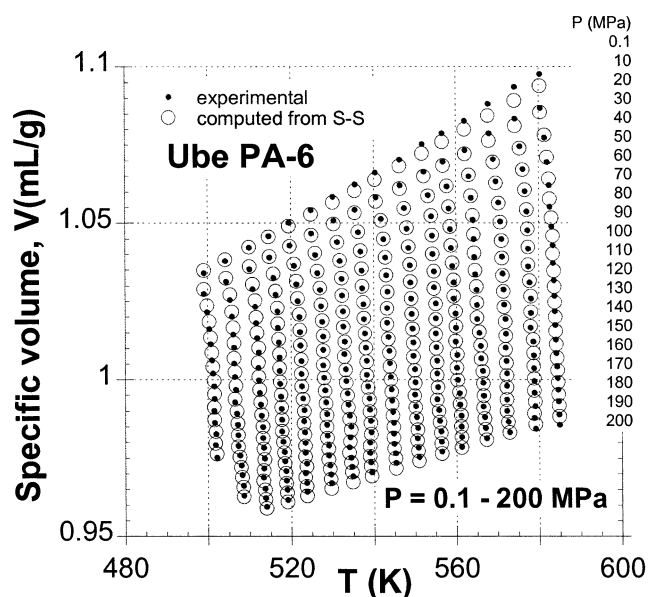
Figure 3. Comparison of experimental (solid circles) and theoretical (open circles) isobars of PA-6 at indicated pressures.

Figure 4. Comparison of experimental (solid circles) and theoretical (open circles) isobars of PNC at indicated pressures.

scaling or reducing parameters of the eos, P^*, V^*, T^*, and the molar mass of the segment, M_s, calculated from the relation

$$(P^*V^*/T^*)M_s = Rc/s = R/3 \tag{10}$$

that follows from the definitions, eq 1. Note that, except for PA, the parameters for other systems are averages. The last two rows give the values of the interaction parameters. Thus, again, for PA the intersegmental interactions, ϵ_{11}^* and v_{11}^* are given, whereas for the two other systems only the averages, $\langle \epsilon^* \rangle$ and $\langle v^* \rangle$, were computed from eq 1. In the next key step these averages must be decomposed into individual contributing interaction parameters. To accomplish this task, the pro-

Table 1. Statistics of Fitting the Eos to Experimental Data and the Computed Parameters for PA, PNC, and Their 1:1 Mixture

parameter	PA	PA:PNC = 1:1	PNC
correlation coeff squared, r^2	0.999999	0.999998	0.999998
standard deviation of data, σ	0.00112	0.00145	0.00127
coeff of determination, CD	0.998602	0.998501	0.998550
P^* (bar)	12574 ± 82	11857 ± 111	11639 ± 126
T^* (K)	11134 ± 32	11364 ± 49	11307 ± 54
$10^4 V^*$ (mL/g)	8919.3 ± 9.6	8943.1 ± 14.3	8888.6 ± 16.2
M_s (g/mol)	27.512	29.700	30.288
ϵ_{11} (kJ/mol)	$\epsilon_{11}^* = 31.23 \pm 0.09$	$\langle \epsilon^* \rangle = 31.49 \pm 0.29$	$\langle \epsilon^* \rangle = 31.71 \pm 0.15$
v_{11} (mL/mol)	$v_{11}^* = 24.54 \pm 0.03$	$\langle v^* \rangle = 26.56 \pm 0.36$	$\langle v^* \rangle = 26.92 \pm 0.05$

Table 2. Molar and Site Fractions for the Matrix in PA-6, PNC, and Their 1:1 Mixture

parameter	PA-6	PA-6/PNC = 1:1	PNC
mole fraction, x_1	1.0000	0.951599	0.902412
site fraction, X_1	1.0000	0.059689	0.028991

posed HCP model will be applied to eq 8. However, first the site fractions, X_i, for the constituents need to be calculated.

An average dry clay platelet is assumed to be a circular disk with diameter $d = 100$ nm and height $h = 1$ nm. Its "molecular" mass, M_p, with a density, $\rho = 2.5$ g/mL, equals $M_p = N_A \rho \pi d^2 h / 4 = 11\,824$ kg/mol, and "molecular" volume $V_p = M/\rho = 4.73 \times 10^6$ mL/mol. The model assumes that the dispersed phase is a clay platelet with 12 nm thick solid layers of PA-6 dispersed in PA-6 matrix whose molar fraction, x_1, is reduced by the amount solidified on the clay platelet:

$$x_1 = \frac{(m_1/M_1) - (m_{1\text{solid}}/M_1)}{(m_1/M_1) + (m_2/M_2)} \qquad (11)$$

where m_1 is the weight fraction of PA-6, $m_{1\text{solid}} = m_2$-$(12/0.96)(1.2/2.5) = 6m_2$ is the weight fraction of PA-6 solidified on the clay (with density $\rho = 1.2$ g/mL, as determined for crystalline polymer), m_2 is the weight fraction of clay, and M_{si} is the molecular weight of statistical segment of component "i", defined as $M_{si} = M_i/s_i$ (M_i and s_i are molecular weight and number of statistical segments, respectively). For neat PA the value $M_{s1} = 27.512$ (cited in Table 1) was computed directly from the reducing parameters (see eq 10). Thus, since the molecular weight of PA is $M_n = 22$ kg/mol, the number of statistical segments $s_1 = 800$. Next, M_{s2} and s_2 have to be calculated for HCP.

According to the hole–lattice theory, a hard-core volume of a statistical segment occupies each lattice site. For the assumed 6–12 potential the factor $2^{1/6}$ relates the positions of potential minimum and onset of repulsion. Thus, for PA $v_{\text{hard}}^* = M_s V^* / 2^{1/2} = 17.35$ mL/mol.

In a mixture, the hard-core volumes of the constituents should not differ too much. However, eq 8 requires that not all v_{ij}^* are identical to each other. In the previous communication[2] $v_{11}^* = v_{22}^*$ was assumed, which lead to $v_{12}^* = 1.4 v_{11}^*$. Such a high value is difficult to accept. Accordingly, in the present computations the ratio $v_{22}^*/v_{11}^* = 1.1$ was used, following work by Papazoglou et al.[20] Hence, $s_2 = V_\rho/(1.1 v_{\text{hard}}^*) = 2.4784 \times 10^5$. Substituting these numbers into eqs 11 and 9 gives respectively the molar and site fractions for PA, PNC, and their 1:1 mixture, as are listed in Table 2.

The "12" parameters characterizing the hetero contacts are approximated by averages—the repulsive

volume by algebraic average of the radii, the attractive interactions by Berthelot's geometric mean rule,[21] i.e.

$$v_{12}^* = [v_{12}^{1/3} + v_{22}^{1/3}]^3/8 \qquad (12)$$

$$\epsilon_{12}^* = (\epsilon_{11}^* \epsilon_{22}^*)^{1/2} \qquad (13)$$

According to the adopted HCP model, in PA there are only free macromolecules characterized by their bulk properties. In the PA/PNC = 1:1 mixture the weight fraction of inorganic component is low enough, $m_2 = 0.008$, for some PA macromolecules to have bulk mobility. However, in PNC the PA macromolecules are all located either in the solidified or in the intermediate layer. In the case of the three examined systems, the matrix changes from one to the other; thus, ϵ_{11}^*, ϵ_{12}^*, v_{11}^*, and v_{12}^* are expected to be different in each, while as assumed $v_{22}^* = 1.1 v_{11}^*$. Since HCP are present in the PNC and PA/PNC = 1:1 systems one may postulate that for these two compositions ϵ_{22}^*, $v_{22}^* = $ constant.

For the two exponents in eq 8 ($p = 2, 4$) there are six parameters. The value of $v_{22}^* = 1.1 v_{11}^*$ was assumed; hence, from eq 12 $v_{12}^* = 1.04921 v_{11}^*$, and ϵ_{12}^* can be calculated from eq 13. This means that only two parameters, ϵ_{11}^*, ϵ_{22}^*, need to be computed from the experimental $\langle \epsilon^* \rangle$ and $\langle v^* \rangle$ data. However, of these two only ϵ_{22}^* is constant, as the matrices of the two polymeric systems are fundamentally different. Considering next the PA/PNC = 1:1 and PA systems, and substituting the computed value of ϵ_{22}^*, the average energetic interaction in the PA matrix, ϵ_{11}^*, is obtained. These values refer to an average matrix, characteristic of the particular clay content. Results of the calculations are presented in Table 3 and Figure 5.

VII. Discussion

The results of extensive *PVT* measurements in two laboratories have been fitted to the Simha–Somcynsky eos. Influences of the experimental procedure were examined. Owing to hygroscopicity, thermal and hydrolytic degradability, variability in the crystalline content, and morphology of the samples, these systems are difficult to measure with the precision required for reliable determination of the thermodynamic parameters. The final set of fitting variables in Table 1 is not an average of several runs, but that for most reliable individual runs, which best describe the true material behavior for each composition. The reliability was judged adequate when the computed hole fraction, $h = h(p,T)$ superimposed for at least three runs with error smaller than 0.1%.

From the point of view of polymer processing, it was interesting to see that extrusion (in TSE with high-

Table 3. Interaction Parameters in PA, PNC, and Their 1:1 Mixture[a]

system contacts	PA-6		PA/PNC = 1:1		PNC	
	ϵ_{ij}^* (kJ/mol)	v_{ij}^* (mL/mol)	ϵ_{ij}^* (kJ/mol)	v_{ij}^* (mL/mol)	ϵ_{ij}^* (kJ/mol)	v_{ij}^* (mL/mol)
11	31.23	24.54	31.21	24.54	(26.69)	24.54
12			31.53	25.75	(29.16)	25.75
22			31.86	26.99	31.86	26.99
X_1	1.000		0.059689		0.028991	

[a] In the PA/PNC mixture and in PNC the variations of v_{ij}^* are as postulated in the text. Values of ϵ_{ij}^* in parentheses were computed for matrices of different mobility; hence, they are fitting averages. The experimental error for ϵ_{ij}^* and v_{ij}^* is ±1.5% and ±1.0%, respectively.
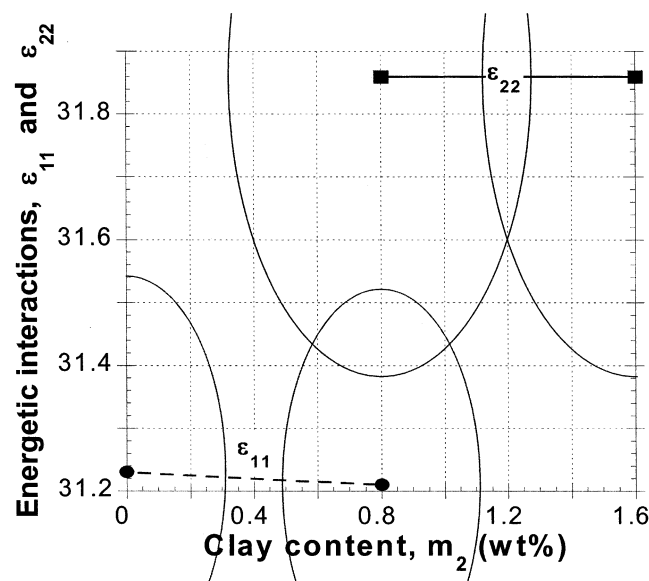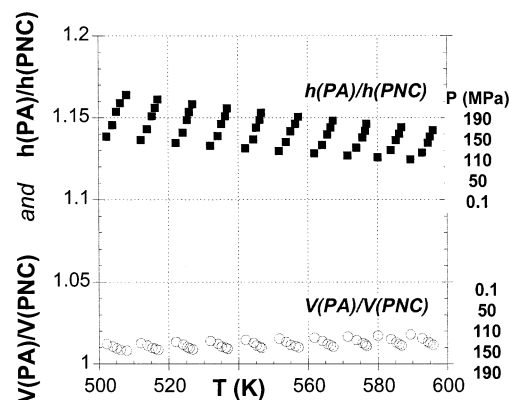

Figure 5. Energetic interaction parameters for the three studied PA/PNC systems. Points are computed from the *PVT* reducing parameters; the arches represent the experimental errors.

Figure 6. *V* and *h* data plotted as ratios at the same *T* and *P* (for each data point). Note that the ratios of *h* increase with *P*, while those of *V* slightly decrease. For the sake of clarity, only data points for five *P* are presented.

shear screw configuration and residence time of ca. 2 min) did not affect the *PVT* behavior of either PA-6 or PNC. However, the rheological measurements on these samples showed that extrusion introduced only a minor change in the flow behavior of neat PA, but it did reduce *G'* and *G''* of the PNC by 74% and 20%, respectively.[19] The changes were most likely related to modification of morphology (breaking of HCP aggregates), but not to hydrolytic or oxidative degradation. Thus, the reported *PVT* behavior of the three compositions describes not only the behavior of virgin resins as supplied by the manufacturer but also that of the materials during and after processing.

To extract the thermodynamic parameters from *PVT* data, a computer program fitted the coupled eqs 5 and 6 to the full set of data by simultaneous optimization of the reducing parameters by the nonlinear least-squares procedure. To speed up the computations, these were carried out in two stages: (1) rapid (seconds) convergence was obtained using the polynomial eq 7, and then (2) using the values of the reducing parameters determined at the first stage, further refinement of values was rapidly obtained by fitting to eqs 5 and 6.

The S–S eos was found to describe well the observed *PVT* behavior. However, as evident in Figures 3 and 4, systematically a few data points at highest temperatures and lowest pressures deviated from the expected behavior. Since these deviations were small (<0.2%) and systematic for all the PA-based systems, they were not taken as a sign of theoretical inadequacy. They could be considered a sign of progressive degradative generation of volatiles during the isothermal runs.

Probably the most important finding reported in the preliminary publication[2] was an unexpectedly large difference of the hole fractions between PA and PNC. The new set of data is presented in Figure 6 in the form of ratios of specific volumes and hole fractions:

$$V(PA)/V(PNC)|_{P,T=\text{const}}; \quad h(PA)/h(PNC)|_{P,T=\text{const}}$$

The incorporation of 1.6 wt % of clay in PA-6 reduced its specific volume by 1–1.5% at $T = 500–595$ K in the full range of $P = 0.1–200$ MPa. At the same time, the clay caused significant reduction of the hole fraction (which is a measure of free volume). As evident from data in Figure 6, the ratio $h(PA)/h(PNC)|_{P,T=\text{const}} = 1.12–1.16$ for $T = 589–508$ K and $P = 0.1–190$ MPa. This is an impressive effect (equivalent to a decrease of melt temperature by ca. 60 °C), especially since it is caused by addition of 0.64 vol % of nanoparticles. However, one may comprehend this behavior considering that in 1 g of PNC there are 8 million platelets with the surface area of about 13 m² capable to "solidify" ca. 9% of the matrix and reduce mobility (hence the free volume) of the rest.

The proposed "hairy" clay platelet (HCP) model not only explains the significant reduction of the free volume in molten PA-6 but also offers a consistent basis for the interpretation of interactions within the clay-containing systems. The model considers that these systems can be viewed as suspensions of solid particles in the matrix of polymer whose mobility and hence properties depend on composition. The solid particle is an exfoliated clay platelet uniformly covered by a 6 nm thick layer of solidlike PA-6, the HCP. The matrix is composed of two types of macromolecules: those that form a ca. 100 nm thick envelope around HCP and free (of HCP influence) PA-6 molecules. According to simple geometric argument, to have any free PA-6 molecules in the system, the organoclay concentration must be below 1.2 wt %.

Thus, in the three systems investigated in this work, PA-6 had only "free" macromolecules, PNC only "not-free" ones, and their 1:1 mixture a combination of these two.

Analysis of the average interaction parameters, $\langle \epsilon^* \rangle$ and $\langle v^* \rangle$, in terms of eq 8 gave a reasonable value of the energetic interaction parameters: $\epsilon_{11}^* = 31.2 \pm 0.5$ and $\epsilon_{22}^* = 31.9 \pm 0.5$—the former is the interaction between statistical segments of "free" PA-6 macromolecules the latter that between the HCP particles. The magnitude of the interaction energies is quite similar as they are related to the surface energy of molten PA-6 and that "solidified" on the outer surface of the HCP particles. The small variation could be expected considering the temperature-reducing parameters in Table 1, viz. $T^* = zq\epsilon^*/Rc = 11\,134 \pm 32$, $11\,364 \pm 49$, and $11\,307 \pm 54$ for PA, PA/PNC = 1:1, and PNC, respectively.

In principle, the current model can readily be modified for a position-dependent matrix system. However, considering the relatively small differences of the interaction parameters for the three materials and the error margin (of the measurements as well of the several computational steps involved in the calculations), this does not seem reasonable.

The proposed model of the PA-6-based clay nanocomposites is far from being general. The PNC considered is characterized by direct end-tethering of PA-6 chains to the clay surface. Owing to its polar nature, PA is also known for good adhesion to silica-based fillers, e.g., to glass fibers. The system is not "contaminated" by other, small organic molecules, e.g., intercalants, which could hinder the clay–polymer interactions.

To compare the *PVT* behavior of such a well-known, exemplary nanocomposite as that used in this work with a poorly dispersed, not end-tethered one, *PVT* measurements are at present carried out on polystyrene containing up to 20 wt % of a commercial organoclay. Owing to the wide range of composition, it is expected that larger variations in the value of the P^*, V^* and T^* parameters will be found. However, as these PS-based nanocomposites have the organic intercalant layer between clay and matrix, the model proposed in this work may not be applicable—Nature will deliver the verdict in a few months.

VIII. Summary and Conclusions

1. The Simha–Somcynsky lattice–hole theory provides a good description of the *PVT* behavior of PA-6 (PA), its clay-reinforced nanocomposite (PNC), and their 1:1 mixture. The correlation coefficient squared, $r^2 \geq 0.999\,998$, and standard deviation of data, $\sigma < 0.0015$ mL/g.

2. Addition of 1.6 wt % (or 0.64 vol %) of exfoliated clay to PA-6 reduces the free volume function h by 12–16% (depending on P and T). This disproportionately large effect suggests that PA-6 chains are adsorbed on the solid surface. The first few adsorbed layers are immobilized, and this loss of mobility translates into a free volume loss.

3. The large specific surface area of exfoliated clay determines matrix mobility and thus influences PNC behavior. In this manner the free volume connection makes *PVT* measurements and their evaluation a key for understanding and predicting PNC behavior.

4. The "hairy clay platelet" (HCP) model is consistent with the significant reduction of the free volume in molten PA-6 and offers a consistent basis for the interpretation of interactions within the clay-containing PA systems. These systems are viewed as a suspension of solid particles in the matrix of polymer whose mobility depends on composition. The solid particle is an exfoliated clay platelet uniformly covered on all sides by a 6 nm thick layer of solidlike PA-6, the HCP. The matrix is composed of two types of macromolecules: those that form a ca. 100 nm thick envelope around HCP and "free" PA-6 molecules with the neat-PA chain mobility.

5. The derived values of the interaction parameters are consistent with expected relative magnitudes. The HCP–HCP interaction parameter, $\epsilon_{22}^* = 31.9 \pm 0.5$, is comparable to the segment–segment interaction parameter in PA matrix, $\epsilon_{11}^* = 31.2 \pm 0.5$. This is consistent with the relative magnitude of the temperature-reducing parameter, $T^* \propto \epsilon^*$, obtained directly by fitting *PVT* data to the eos.

6. In accord with the lattice model, it was assumed that a statistical segment of PA macromolecule or that of HCP occupies the lattice site. The size of these segments was related, viz. $v_{11}^* = v_{22}^*/1.1$, where $v_{11}^* = 24.54$ mL/mol is the value measured for neat PA segment–segment repulsive volume interaction. Furthermore, it was assumed that the "12" hetero interactions, v_{12}^* and ϵ_{12}^*, are given by appropriate averages: for the repulsive volume, $v_{12}^* = [(1 + 1.1^{1/3})/2]^3 v_{11}^* \cong 1.04921 v_{11}^*$, whereas for the interaction energy $\epsilon_{12}^* = (\epsilon_{11}^* \epsilon_{22}^*)^{1/2}$.

References and Notes

(1) Rodgers, P. A. *J. Appl. Polym. Sci.* **1993**, *48*, 1061; *50*, 2075.
(2) Simha, R.; Utracki, L. A.; Garcia-Rejon, A. *Compos. Interfaces* **2001**, *8*, 345.
(3) Simha, R.; Somcynsky, T. *Macromolecules* **1969**, *2*, 342.
(4) Okada, A.; Usuki, A. *Mater. Sci. Eng.* **1995**, *C3* (2), 109.
(5) Utracki, L. A.; Simha, R. *Macromol. Chem. Phys., Mol. Theory Simul.* **2001**, *10*, 17.
(6) Jain, R. K.; Simha, R. *Macromolecules* **1980**, *13*, 1501.
(7) Fleer, G.; Cohen-Stuart, M. A.; Scheutjens, J. M. H. M.; Cosgrove, T. Vincent, B. *Polymers at Interfaces*; Chapman and Hall: London, 1993.
(8) Cosgrove, T.; Heath, T. G.; Ryan, K.; Crowley, T. L. *Macromolecules* **1987**, *20*, 2879.
(9) Cosgrove, T.; Heath, T. G.; Phipps, J. S.; Richardson, R. M. *Macromolecules* **1991**, *24*, 94.
(10) Israelachvili, J. N.; Tirrell, M.; Klein, J.; Almog, Y. *Macromolecules* **1984**, *17*, 204.
(11) Horn, R. G.; Israelachvili, J. N. *Macromolecules* **1988**, *21*, 2836.
(12) Luengo, G.; Schmitt, F.-J.; Hill, R.; Israelachvili, J. N. *Macromolecules* **1997**, *30*, 2482.
(13) Hu, H.-W.; Granick, S. *Science* **1992**, *258*, 1339.
(14) Hentschke, R. *Macromol. Theory Simul.* **1997**, *6*, 287.
(15) Okada, A.; Fukushima, Y.; Kawasumi, M.; Inagaki, S.; Usuki, A.; Sugiyama, S.; Kurauchi, T.; Kamigaito, O. US Pat., 4,739,007, 1988.04.19, Appl. 1985.09.30, to Kabushiki Kaisha Toyota Chuo Kenkyusho.
(16) Usuki, A.; Kawasumi, M.; Kojima, Y.; Fukushima, Y.; Okada, A.; Kurauchi, T.; Kamigaito, O. *J. Mater. Res.* **1993**, *8*, 1179.
(17) Ube Industries, Ltd., Nylon Resin Department High Performance Nylon Resin–Technical Data March, 2000.
(18) Deguchi, R.; Nishio, T.; Okada, A. US Pat. 5,102,948, 07.04.1992, Appl. 02.05.1990; EP 398 551 B1, 15.11.1995, Appl. 02.05.1990, to Ube Industries, Ltd., and Toyota Jidosha Kabushiki Kaisha, Aichi, Japan.

(19) Utracki, L. A.; Lyngaae-Jørgensen, J. *Rheol. Acta* **2002**, *41,* 394.

(20) Papazoglou, E.; Simha, R.; Maurer, F. H. J. *Rheol. Acta* **1989**, *28*, 302.

(21) Simha, R.; Xie, H. *Polym. Bull. (Berlin)* **1998** *40*, 329.

MA0215464